

See discussions, stats, and author profiles for this publication at: <https://www.researchgate.net/publication/23892085>

Ultraviolet Imaging Telescope images of the reflection nebula NGC 7023 – Derivation of ultraviolet scattering properties of dust grains

Article in *The Astrophysical Journal* · September 1992

DOI: 10.1086/186475 · Source: NTRS

CITATIONS

78

READS

43

7 authors, including:



Adolf N. Witt

University of Toledo

239 PUBLICATIONS 7,075 CITATIONS

[SEE PROFILE](#)

Some of the authors of this publication are also working on these related projects:



DIB - ERE connection [View project](#)



Red Rectangle [View project](#)

ULTRAVIOLET IMAGING TELESCOPE IMAGES OF THE REFLECTION NEBULA NGC 7023: DERIVATION OF ULTRAVIOLET SCATTERING PROPERTIES OF DUST GRAINS

ADOLF N. WITT,¹ JENS K. PETERSOHN,¹ RALPH C. BOHLIN,² ROBERT W. O'CONNELL,³ MORTON S. ROBERTS,⁴
 ANDREW M. SMITH,⁵ AND THEODORE P. STECHER⁶

Received 1992 March 31; accepted 1992 May 14

ABSTRACT

The Ultraviolet Imaging Telescope, as part of the *Astro-1* mission, was used to obtain high-resolution surface brightness distribution data in six ultraviolet wavelength bands for the bright reflection nebula NGC 7023. From the quantitative comparison of the measured surface brightness gradients, ratios of nebular to stellar flux, and detailed radial surface brightness profiles with corresponding data from the visible, two major conclusions result: (1) the scattering in the near- and far-ultraviolet in this nebula is more strongly forward-directed than in the visible; (2) the dust albedo in the ultraviolet for $\lambda \geq 140$ nm is identical to that in the visible, with the exception of the 220 nm bump in the extinction curve. In the wavelength region of the bump, the albedo is reduced by 25% to 30% in comparison with wavelength regions both shorter and longer. This lower albedo is expected, if the bump is a pure absorption feature.

1. INTRODUCTION

NGC 7023 is one of the brightest and most frequently studied reflection nebulae. A complete mapping of the surface brightness of this object over a wide range of wavelengths in visible and ultraviolet spectral regions offers an excellent opportunity to derive the wavelength dependence of the scattering properties of the nebular dust. Such information provides constraints for models of interstellar grains and helps define the continuum opacity of interstellar space in the visible and the UV.

The unique contribution of the Ultraviolet Imaging Telescope (UIT) to this investigation consisted of its ability to record the extended surface brightness distribution of NGC 7023 in a series of six UV wavelength bands, allowing the direct determination of surface brightness gradients in the UV in this object for the first time. The variation of the surface brightness gradient in NGC 7023 with wavelength is a particularly clear indicator of the wavelength dependence of the asymmetry of the scattering phase function, because the illuminating star HD 200775 is well-embedded in an optically thick nebula. The optical depth of dust in front of HD 200775 in the UV is typically twice as large as in the visible (Walker et al. 1980). Hence, given comparable albedos in the two regions, multiple scattering grows with increasing angular offset from the star. (Witt & Oshel 1977). Consequently, a less steep surface brightness gradient would be expected in the UV, if the phase function asymmetry remained unchanged from its value in the visible. This effect would be strengthened further, if the scattering were less forward-directed in the UV compared with the visible. By contrast, a more strongly forward-directed phase function in the UV would result in a steeper surface brightness

gradient there, which could more than balance the expected optical depth effect. Such a clear distinction is desirable, because two recent studies of diffuse far-ultraviolet radiation at high galactic latitudes concluded that the galactic background requires either low-albedo, isotropically scattering dust (Hurwitz, Bowyer, & Martin 1991) or high-albedo, strongly forward-scattering dust (Onaka & Kodaira 1991). Provided that the dust in NGC 7023 is representative of typical interstellar grains, the UIT observations of NGC 7023 are a key to demonstrating that the dust has a high albedo and is strongly forward-scattering in the UV.

2. OBSERVATIONS

Eighteen exposures in six UIT filter bands were obtained of NGC 7023, with exposure times ranging from 13.1 to 582 s. The six deepest exposures listed in Table 1 are used for the analysis of the nebular brightness distribution. The data reduction and calibration procedures applied to the raw data are described by Stecher et al. (1992). Values for the flux of the illuminating star, HD 200775, are derived from archival *IUE* observations by convolving the stellar spectral energy distribution with the UIT instrumental response functions of our six bands (Stecher et al. 1992), and the results are listed in column (7) of Table 1. All surface brightness measurements in NGC 7023 involve subtraction of the sky background, and results are in units of $S/F_*[\text{sr}^{-1}]$, where S is the nebular intensity and F_* is the flux observed from HD 200775. Figure 1 (Plate L2) shows the result of a 546 s exposure of NGC 7023 with the near-UV A1 filter, with a superposed set of isophotes. The outermost isophote corresponds to a relative surface brightness of $\log(S/F_*) = 4.0[\text{sr}^{-1}]$, and additional isophotes show increasing values in steps of 0.2 in $\log(S/F_*)$.

Table 1 contains relevant data about the six UIT images used for this analysis. As a measure of the nebular surface brightness, column (5) has the relative intensity $\log(S/F_*)$ at an offset of $100''$ from the illuminating star, averaged over an $11''.4$ wide annulus. Column (6) lists the nebular flux integrated between offsets of $34''$ and $170''$ and divided by the corresponding flux from HD 200775. The two boundaries are defined by the extent of the point spread function of the overexposed central star, which contaminates the image for $r \leq 30''$, and by

¹ Ritter Astrophysical Research Center, University of Toledo, Toledo, OH 43606.

² Space Telescope Science Institute, Homewood Campus, Baltimore, MD 21218.

³ Astronomy Department, University of Virginia, P.O. Box 3818, Charlottesville, VA 22903.

⁴ National Radio Astronomy Observatory, Edgemont Road, Charlottesville, VA 22903.

⁵ NASA Goddard Space Flight Center, Code 681, Greenbelt, MD, 20771.

⁶ NASA Goddard Space Flight Center, Code 680, Greenbelt, MD, 20771.

PLATE L2

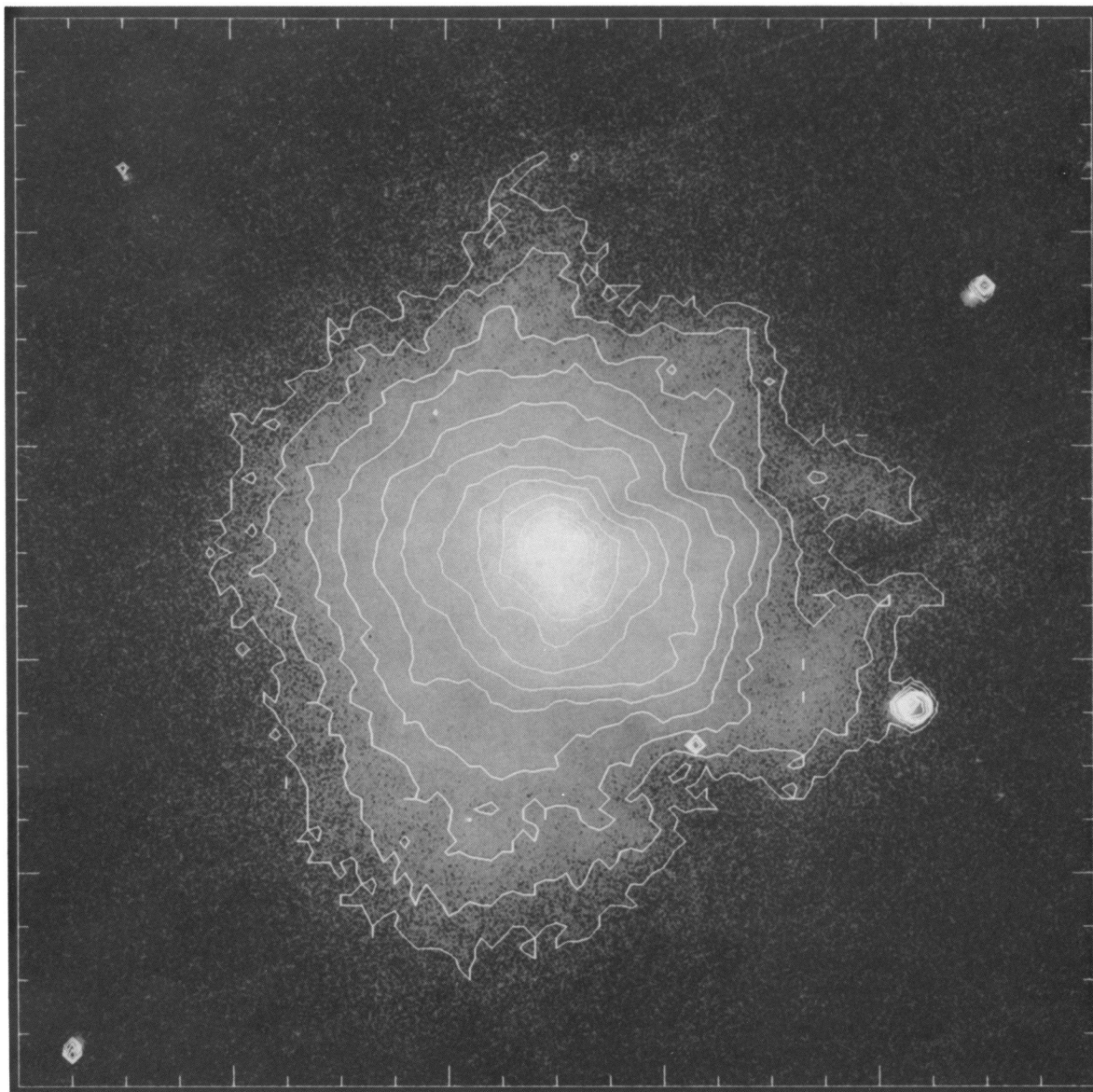


FIG. 1.—UIT image of NGC 7023 from 546 s exposure with the A1 filter. North is at the top and east is to the left. The displayed image has dimensions of $1364'' \times 1364''$. Superposed is a set of isophotes in steps of 0.2 in units of $\log (S/F_{\star})$. The outermost isophote corresponds to $\log (S/F_{\star}) = 4.0 \text{ (sr}^{-1}\text{)}$.

WITT et al. (see 395, L5)

TABLE 1
ULTRAVIOLET IMAGING TELESCOPE IMAGES OF NGC 7023

Image Number (1)	Filter (2)	Peak λ (nm) (3)	Exposure (s) (4)	$\log (S/F_*)_{100''}$ (sr^{-1}) (5)	$(F_N/F_*)_{34''-170''}$ (6)	F_* (ergs $\text{cm}^{-2} \text{s}^{-1} \text{\AA}^{-1}$) (7)
NUV 0201	A1	276.3	546	5.37	0.53	3.89×10^{-12}
NUV 0459	A5	250.8	333	5.31	0.47	3.81×10^{-12}
NUV 0453	A4	218.4	582	5.26	0.46	2.93×10^{-12}
NUV 0456	A2	185.3	235	5.42	0.63	4.52×10^{-12}
FUV 0211	B5	151.8	546	5.50	0.76	6.26×10^{-12}
FUV 0214	B1	144.3	546	5.50	0.76	5.82×10^{-12}

the poor detection of outer nebular regions at $r > 170''$ on the two shortest exposures, NUV 0456 and NUV 0459. The integrated nebular fluxes in Table 1 for the limited range $34''-170''$ are lower limits to the total nebular fluxes, which in the case of the well-exposed images are about 50% larger. These integrated nebular fluxes for NGC 7023 are in good agreement with the *ANS* and the *TD-1* results reported by Witt et al. (1982).

3. ANALYSIS

3.1. Surface Brightness Gradients

The surface brightness of NGC 7023 is one of the highest found among reflection nebulae, and is close to the theoretical maximum, which can occur for forward-scattering grains only if the illuminating star is embedded in the nebula at an optical depth of about unity. In such a geometry, the wavelength dependence of the surface brightness gradient yields direct information about the wavelength dependence of the phase function asymmetry.

As shown by Witt et al. (1982), the surface brightness distribution of NGC 7023 is described by a power law of the form

$$S(r) \propto r^{-p}, \quad (1)$$

where r is the angular offset from the central illuminating star. We determined representative values of $S(r)$ by averaging the recorded surface brightness in a series of concentric annuli of $11''.4$ width, centered on HD 200775. Power law fits are made for the data within the radial offset range $34'' \leq r \leq 170''$, which are the limits discussed above in § 2. Results for our three most deeply exposed UIT images are listed in Table 2, where p -values from ground-based observation of NGC 7023 by Witt & Cottrell (1980) are given for comparison. The latter were derived from the observations in the offset range $30'' \leq r \leq 175''$. We find the surface brightness gradients to be essentially constant with wavelength. However, the small trend toward increasing p -values among the UIT data sets is marginally significant in view of the extreme consistency in the observing and analysis techniques applied to the UIT data.

TABLE 2
POWER-LAW FITS AND RATIOS OF NEBULAR-TO-STELLAR
FLUX IN NGC 7023

Filter (1)	Peak λ (nm) (2)	p (3)	$(F_N/F_*)_{0''-300''}$ (4)
<i>y</i>	551.5	1.54 ± 0.03	0.41 ± 0.02
<i>b</i>	473.3	1.52 ± 0.03	0.43 ± 0.02
<i>v</i>	409.3	1.49 ± 0.03	0.54 ± 0.03
UIT:A1	276.3	1.50 ± 0.02	0.91 ± 0.05
UIT:B5	151.8	1.54 ± 0.02	1.19 ± 0.05
UIT:B1	144.3	1.60 ± 0.02	1.21 ± 0.06

We have used the geometrical model of NGC 7023 of Witt et al. (1982) for an estimate of the range of values of the phase function asymmetry which is implied by the observed surface brightness gradients. Figure 2 plots the expected value of p as a function of the asymmetry parameter g of the Henyey-Greenstein phase function for $\tau = 0.77$, corresponding to the *v*-band ($\lambda = 409.3$ nm), and for $\tau = 1.25$, corresponding to the UIT:B1 band ($\lambda = 141.3$ nm). Also shown as dashed lines are the limiting values of the observed range of p -values, 1.49 and 1.60. The small shaded area bounded by these four curves defines the derived range of g -values, $0.67 \leq g \leq 0.76$. The increase of p with decreasing wavelength in the UIT bands, which occurs despite an increase in optical depth (Walker et al. 1980), leads us to conclude that the phase function becomes increasingly forward-directed with decreasing wavelength in the UV, with an upper limit near $g = 0.8$.

3.2. The Dust Albedo

The overall scattering efficiency of the nebular dust may be estimated from the ratio of the total nebular scattered flux to the direct stellar flux observed at Earth. Table 2 lists this ratio for three wavelengths in the visible and for the three most deeply imaged UIT bands in column (4). In all cases the range of nebular flux integration is $0'' \leq r \leq 300''$, after corrections for the spread of the overexposed stellar image were applied.

For simple principles of radiative transfer we obtain the approximation

$$F_N/F_* \propto a^m(1 - e^{-\tau})e^{\tau} \quad (2)$$

where a is the albedo, τ is the optical depth at which the star is

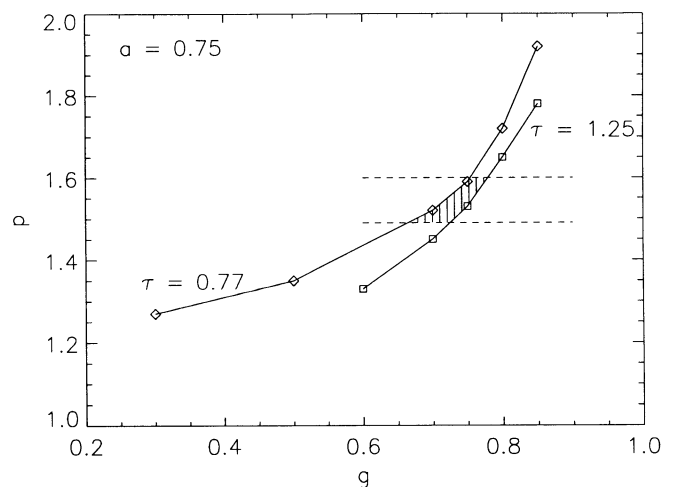


FIG. 2.—Predicted relationships between the surface brightness power-law exponent p and the phase function asymmetry g for two optical depths, corresponding to the *v*-band ($\tau = 0.77$) and the UIT:B1 band ($\tau = 1.25$). The two limiting values of the observed p -range are indicated by dashed lines.

embedded, and m is the effective multiplicity of scattering (Witt & Oshel 1977). This approach assumes that the scattering is forward directed and that the phase function asymmetry is not strongly variable with wavelength, two facts already established in the previous section. The value of m is a function of τ and, thus, a function of wavelength. We have determined representative multiplicity values from Monte Carlo scattering models for $\tau = 0.77$ and $\tau = 1.25$, the respective optical depths for the v -band and the UIT:B1 band, and we find $m(\tau = 0.77) = 1.36$, $m(\tau = 1.25) = 1.64$. These values assume $g = 0.75$. Using the extinction curve determined for HD 200775 by Walker et al. (1980) as representative for NGC 7023, equation (2) and the results in Table 2 imply that the far-UV dust albedo must be nearly identical in value to the albedo in the visible. This conclusion is derived from general principles of radiative transfer and is not based on any specific model.

3.3. Radiative Transfer Models

With the availability of detailed UV-surface brightness distributions for NGC 7023 from UIT, new tests of the specific radiative transfer model for NGC 7023 of Witt et al. (1982) are possible. This model assumes a spherically symmetric nebula with a centrally embedded star. The physical radius of 1 pc corresponds to a visual optical depth of 0.54; and the nebular density declines with distance from the star as $r^{-0.26}$, after being constant for the initial 0.01 pc. The distance from the Earth is taken as 350 pc. The Henyey-Greenstein phase function allows for anisotropic scattering, and multiple scattering is taken into account. The scaling of the nebular optical depth in the UV is based on the UV extinction curve for HD 200775 (Walker et al. 1982). Adjustable parameters are the albedo a , which mainly determines the overall surface brightness level, and the phase function asymmetry g , which most strongly influences the radial surface brightness distribution.

Figure 3 shows the observed radial brightness distributions

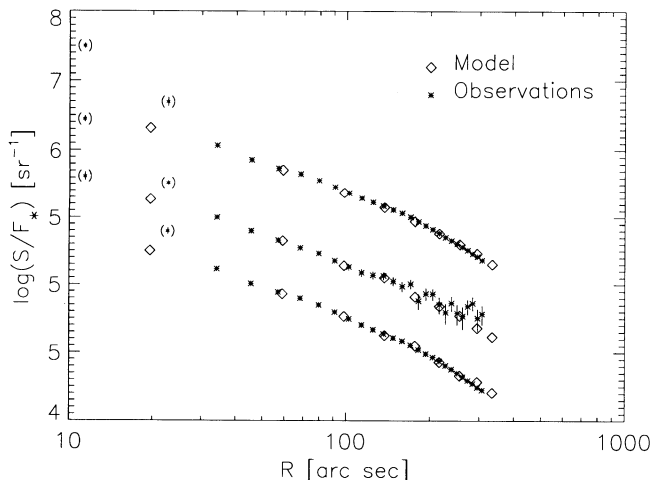


FIG. 3.—Average radial surface brightness profiles of NGC 7023 derived from a 546 s exposure with the UIT:A1 filter (*top*), from a 582 s exposure with the UIT:A4 filter (*middle*), and from a 546 s exposure with the UIT:B1 filter (*bottom*). The second and third data sets are displaced vertically by one and two units in $\log(S/F_*)$, respectively. The two innermost points (in parentheses) of each set are contaminated by the spreading image of the overexposed central star, and are not included in the comparison with the models. The error bars, representing three standard deviations of the mean, are in most cases smaller than the symbol size.

of NGC 7023, obtained with the A1 filter (*top*), the A4 filter (*middle*), and the B1 filter (*bottom*). The second and third set of observations are displaced vertically by one and two units in $\log(S/F_*)$, respectively. Each observational point represents the mean surface brightness found in circular annuli of $11''.4$ width, and error bars equal to three standard deviations of the mean are shown, wherever they exceed the size of the symbols themselves. The first two observational points of each set, shown in parentheses, are contaminated by the spread of the overexposed central star and are excluded from the comparison with the models.

The model fits are achieved for the A1-data with $\tau = 1.04$, $a = 0.72$, and $g = 0.70$. The A4-data (220 nm) require $\tau = 1.30$, $a = 0.52$, $g = 0.70$. Finally, the B1-data are fit with $\tau = 1.25$, $a = 0.74$, $g = 0.75$. The reduction of the albedo near 220 nm is consistent with the absorption nature for the 220 nm bump in the extinction curve (Lillie & Witt 1976); it is also visibly demonstrated by the *downward* displacement of the A4-data with respect to the central position between the A1-data and the B1-data in Figure 3.

4. DISCUSSION

The most important result derived from the UIT observations of NGC 7023 is the clear indication of a strongly forward-scattering phase function for the nebular grains in the UV, and by inference, for interstellar grains in the UV. While the actual numerical values of the phase function asymmetry parameter g depend to some degree on a specific model, the conclusion that $g(\text{UV}) > g(\text{vis})$ is based on general radiative transfer principles and on the observational data alone. This conclusion represents a significant revision of one of the results of Witt et al. (1982) regarding the scattering in NGC 7023, which was $g(\text{UV}) < g(\text{vis})$. We conclude that detailed surface brightness profiles at all relevant wavelengths are indispensable, if valid conclusions regarding the phase function asymmetry are to be drawn.

Except for a reduction near 220 nm, our finding of a high dust albedo in the UV confirms the earlier result of Witt et al. (1982). The conclusion that $a(\text{UV}) \approx a(\text{vis})$ has been based on the high observed ratio of nebular to stellar flux in NGC 7023 and its specific variation with wavelength. This specific variation requires that the bulk of the scattering dust is in front of the embedded star. Otherwise, one would conclude $a(\text{UV}) \gg a(\text{vis})$. The high dust albedo in NGC 7023 is only weakly dependent upon the value found for the phase function asymmetry, because the integrated nebular flux is a sum over a wide range of scattering angles. If the phase function were less strongly forward-directed, the associated albedo would need to be increased slightly.

Duley & Williams (1980) suggested that the high far-UV surface brightness of reflection nebulae may be due in part to fluorescence by molecular hydrogen, as in the nebula IC 63 (Witt et al. 1989), where the B0.5 IV pe star γ Cas illuminates a detached cloud under large scattering angles. Consequently, the scattered light intensity in IC 63 is low for forward-scattering grains; and isotropically emitted H_2 fluorescence, favored by the earlier spectral type of the illuminating star, is relatively more important than for NGC 7023. In the case of NGC 7023, the forward-scattering geometry favors the scattered light intensity; and the later spectral type of HD 200775 (B3 V, Baschek et al. 1982) reduces the possibility of radiative excitation of H_2 . No H_2 emission is detected in the *IUE* spectrum of NGC 7023 (SWP 5966) taken at $22''$ offset distance

(Witt et al. 1982). Some of us (A. N. W., R. C. B., T. P. S.) have recently obtained *IUE* spectra at the locations of filaments of extended red emission (ERE) in NGC 7023 and have detected H₂ fluorescence at these locations. At these spatially extremely limited locations, H₂ emission is found to add as much as 40% to the scattered light intensity admitted by the B1 and B5 filters; but averaged over the entire nebula, the H₂ contribution is estimated at less than 10%. Consequently, our far-UV albedo estimates for $\lambda < 200$ nm may need to be reduced to about $a \simeq 0.65$.

5. SUMMARY

The UIT experiment on *Astro-1* has produced 18 photographs in the near and far-UV of the classical reflection nebula NGC 7023, with high spatial resolution, in six different band-

passes. A surface brightness analysis based on the six most deeply exposed images leads to these conclusions:

1. The dust scattering is strongly forward-directed at UV wavelengths. The phase function symmetry factor in the far-UV is estimated as $g \simeq 0.75$, if the corresponding value in the visible is $g \simeq 0.60$ to 0.65 .

2. The dust albedo in the near- and far-UV is at least as high as the albedo in the visible, i.e., $a \simeq 0.65$, even after possible H₂ fluorescence contributions are taken into account. The short-wavelength limit of this study is about 140 nm.

3. The albedo in the 220 nm band is definitely reduced compared to values at both shorter as well as longer wavelengths. The reduction by about 25% to 30% is consistent with a pure absorption nature of the $\lambda 220$ nm extinction bump in the extinction curve of HD 200775, the illuminating star in NGC 7023.

REFERENCES

- Baschek, B., Beltrametti, J., Köppen, J., & Traving, G. 1982, *A&A*, 105, 300
 Duley, W. W., & Williams, D. A. 1980, *ApJ*, 242, L179
 Hurwitz, M., Bowyer, S., & Martin, C. 1991, *ApJ*, 372, 167
 Lillie, C. F., & Witt, A. N. 1976, *ApJ*, 208, 64
 Onaka, T., & Kodaira, K. 1991, *ApJ*, 379, 532
 Stecher, T. P., et al. 1992, *ApJ*, 395, L1
 Walker, G. A. H., Yang, S., Fahlmann, G. G., & Witt, A. N. 1980, *PASP*, 92, 411
 Witt, A. N., & Cottrell, M. J. 1980, *ApJ*, 85, 22
 Witt, A. N., & Oshel, E. R. 1977, *ApJS*, 35, 31
 Witt, A. N., Stecher, T. P., Boroson, T. A., & Bohlin, R. C. 1989, *ApJ*, 336, L21
 Witt, A. N., Walker, G. A. H., Bohlin, R. C., & Stecher, T. P. 1982, *ApJ*, 261, 492